Electrophysiology.

Two-microelectrode voltage-clamp experiments were performed as described[27]. In experiments involving voltage ramping or holding, currents and voltages were digitized at 0.3 or 200 ms per sample and Bessel filtered at 10 or 0.02 kHz, respectively. We calculated ratios of permeability coefficients for monovalent cations using the equation derived from the GHK equation[28]: $P_X/P_{Na} = \exp(\Delta V_r/58.5)$, where ΔV_r (mV) is the change in reversal potential. To estimate the permeabilities of divalent cations relative to that of Na^+ under physiological conditions, we compared cation-evoked currents at −50 mV. Experimental results are expressed as mean ± s.e.m. (n). Patch-clamp experiments were performed as described[29]. We used a pipette-tip resistance of 5–10 MΩ and seal resistance of >10 GΩ. Single-channel currents were measured with an integrating patch-clamp amplifier, digitized at 0.15 ms per sample and filtered at 3 kHz through an 8-pole Bessel filter. To prevent possible run-down, cAMP, GTP-γ-S and ATP (0.1 mM) were added to intracellular solutions in most cases.

^{45}Ca-uptake measurements.

$^{45}CaCl_2$ of 30 and 60 μM, respectively, was added to uptake solutions containing 1 and 5 mM non-radioactive Ca^{2+}. 8–10 oocytes were incubated in 0.5 ml of uptake solution and uptake was terminated by washing oocytes in ice-cold NaCl-containing solution (pH 7.5). For experiments involving voltage-clamped ^{45}Ca uptake, Ca^{2+}-evoked currents and uptake of ^{45}Ca were simultaneously measured[30] at −50 mV.

Received 21 May; accepted 9 July 1999.

1. Gabow, P. A., Autosomal dominant polycystic kidney disease. *N. Engl. J. Med.* **329,** 332–342 (1993).
2. The European Polycystic Kidney Disease Consortium. The polycystic kidney disease 1 gene encodes a 14 kb transcript and lies within a duplicated region on chromosome 16. *Cell* **77,** 881–894 (1994).
3. The International Polycystic Kidney Disease Consortium. Polycystic kidney disease: the complete structure of the PKD1 gene and its protein. *Cell* **81,** 289–298 (1995).
4. Hughes, J. *et al*. The polycystic kidney disease 1 (PKD1) gene encodes a novel protein with multiple cell recognition domains. *Nature Genet.* **10,** 151–160 (1995).
5. Mochizuki, T. *et al*. PKD2, a gene for polycystic kidney disease that encodes an integral membrane protein. *Science* **272,** 1339–1342 (1996).
6. Nomura, H. *et al*. Identification of PKDL, a novel polycystic kidney disease 2-like gene whose murine homologue is deleted in mice with kidney and retinal defects. *J. Biol. Chem.* **273,** 25967–24973 (1998).
7. Wu, G. *et al*. Identification of PDK2L, a human PKD2-related gene: tissue-specific expression and mapping to chromosome 10q25. *Genomics* **54,** 564–568 (1998).
8. Kiselyov, K. *et al*. Functional interaction between InspP3 receptors and store-operated Htrp3 channels. *Nature* **396,** 478–482 (1998).
9. Perez-Reyes, E. *et al*. Molecular characterization of a neuronal low-voltage-activated T-type calcium channel. *Nature* **391,** 896–900 (1998).
10. Xia, X. M. *et al*. Mechanism of calcium gating in small-conductance calcium-activated potassium channels. *Nature* **395,** 503–507 (1998).
11. Jorgensen, A. J., Bennekou, P., Eskesen, K. & Kristensen, B. I. Annexins from Ehrlich ascites cells inhibit the calcium-activated chloride current in *Xenopus laevis* oocytes. *Pflugers Arch.* **434,** 261–266 (1997).
12. Boton, R., Dascal, N., Gillo, B. & Lass, Y. Two calcium-activated chloride conductances in *Xenopus laevis* oocytes permeabilized with the ionophore A23187. *J. Physiol. (Lond.)* **408,** 511–534 (1989).
13. Zitt, C. *et al*. Expression of TRPC3 in Chinese hamster ovary cells results in calcium-activated cation currents not related to store depletion. *J. Cell Biol.* **138,** 1333–1341 (1997).
14. Zuhlke, R. D. & Reuter, H. Ca^{2+}-sensitive desensitization of L-type Ca^{2+} channels depends on multiple cytoplasmic amino acid sequences of the α_{1C} subunit. *Proc. Natl Acad. Sci. USA* **95,** 3287–3294 (1998).
15. Gogelein, H., Dahlem, D., Englert, H. C. & Lang, H. J. Flufenamic acid, mefenamic acid and niflumic acid inhibit single nonselective cation channels in the rat exocrine pancreas. *FEBS Lett.* **268,** 79–82 (1990).
16. Kunze, D. L., Sinkins, W. G., Vaca, L. & Schilling, W. P. Properties of single *Drosophila* Trp1 channels expressed in Sf9 insect cells. *Am. J. Physiol.* **272,** C27–C34 (1997).
17. Gillo, B. *et al*. Coexpression of *Drosophila* TRP and TRP-like proteins in *Xenopus* oocytes reconstitutes capacitative Ca^{2+} entry. *Proc. Natl Acad. Sci. USA* **93,** 14146–14151 (1996).
18. Caterina, M. J. *et al*. The capsaicin receptor: a heat-activated ion channel in the pain pathway. *Nature* **389,** 816–824 (1997).
19. Birnbaumer, L. *et al*. On the molecular basis and regulation of cellular capacitative calcium entry: roles for TRP proteins. *Proc. Natl Acad. Sci. USA* **93,** 15195–15202 (1996).
20. Yang, X. C. & Sachs, F. Block of stretch-activated ion channels in *Xenopus* oocytes by gadolinium and calcium ions. *Science* **243,** 1068–1071 (1989).
21. Lane, J. W., McBride, D. W. Jr & Hamill, O. P. Ionic effects on amiloride block of the mechanosensitive channel in *Xenopus* oocytes. *Br. J. Pharmacol.* **108,** 116–119 (1993).
22. Tzounopoulos, T., Maylie, J. & Adelman, J. P. Induction of endogenous channels by high levels of heterologous membrane proteins in *Xenopus* oocytes. *Biophys. J.* **69,** 904–908 (1995).
23. Sullivan, L. P., Wallace, D. P. & Grantham, J. J. Chloride and fluid secretion in polycystic kidney disease. *J. Am. Soc. Nephrol.* **9,** 903–916 (1998).
24. Tsiokas, L., Kim, E., Arnould, T., Sukhatme, V. P. & Walz, G. Homo- and heterodimeric interactions between the gene products of PKD1 and PKD2. *Proc. Natl Acad. Sci. USA* **94,** 6965–6970 (1997).
25. Qian, F. *et al*. PKD1 interacts with PKD2 through a probable coiled-coil domain. *Nature Genet.* **16,** 179–183 (1997).
26. Saadi, I. *et al*. Molecular genetics of cystinuiria: mutation analysis of SLC3A1 and evidence for another gene in type I (silent) phenotype. *Kidney Int.* **54,** 48–55 (1998).
27. Chen, X.-Z., Shayakul, C., Berger, U. V., Tian, W. & Hediger, M. A. Characterization of a rat Na^+-dicarboxylate cotransporter. *J. Biol. Chem.* **273,** 20972–20981 (1998).
28. Hille, B. in *Ionic Channels of Excitable Membranes* (ed. Hille, B.) 105–108 (Sinauer, Sunderland, Massachusetts, 1992).
29. Hamill, O. P., Marty, A., Neher, E., Sakmann, B. & Sigworth, F. J. Improved patch-clamp techniques for high-resolution current recording from cells and cell-free membrane patches. *Pflugers Arch.* **391,** 85–100 (1981).
30. Chen, X.-Z., Zhu, T., Smith, D. E. & Hediger, M. A. Stoichiometry and kinetics of the rat high-affinity H^+-coupled peptide transporter PepT2. *J. Biol. Chem.* **274,** 2773–2779 (1999).

Acknowledgements

We thank P. Fong for providing pTLN2. X.-Z.C. is a recipient of the International Human Frontier Science Program Long-Term Fellowship. This work is supported by NARSAD and the Stanley Foundation (P.M.V.), the St. Giles Foundation (E.M.B.) and NIH (S.T.R., E.M.B., M.A.H. and J.Z.).

Correspondence and requests for materials should be addressed to J.Z. (e-mail: zhou@rics.bwh.harvard. edu) or M.A.H. (e-mail: mhediger@rics.bwh.harvard.edu).

A polycystic kidney-disease gene homologue required for male mating behaviour in *C. elegans*

Maureen M. Barr & Paul W. Sternberg

Howard Hughes Medical Institute and Division of Biology, California Institute of Technology, Pasadena, California 91125, USA

The stereotyped mating behaviour of the *Caenorhabditis elegans* male is made up of several substeps: response, backing, turning, vulva location, spicule insertion and sperm transfer. The complexity of this behaviour is reflected in the sexually dimorphic anatomy and nervous system[1]. Behavioural functions have been assigned to most of the male-specific sensory neurons by means of cell ablations; for example, the hook sensory neurons HOA and HOB are specifically required for vulva location[2]. We have investigated how sensory perception of the hermaphrodite by the *C. elegans* male controls mating behaviours. Here we identify a gene, *lov-1* (for location of vulva), that is required for two male sensory behaviours: response and vulva location. *lov-1* encodes a putative membrane protein with a mucin-like, serine–threonine-rich amino terminus[3] followed by two blocks of homology to human polycystins, products of the autosomal dominant polycystic kidney-disease loci PKD1 and PKD2 (ref 4). LOV-1 is the closest *C. elegans* homologue of PKD1. *lov-1* is expressed in adult males in sensory neurons of the rays, hook and head, which mediate response, vulva location, and potentially chemotaxis to hermaphrodites, respectively[2,5]. PKD-2, the *C. elegans* homologue of PKD2, is localized to the same neurons as LOV-1, suggesting that they function in the same pathway.

We examined the mating behaviour of existing mutants that are defective in sensory behaviours including mechanosensation, osmotic avoidance and chemotaxis to soluble and volatile odorants. Only males with severe defects in all sensory neuron cilia (*daf-10*, *osm-5*, *osm-6* and *che-3*) were defective of vulva location (Table 1); all cilia in *C. elegans* are in the dendritic endings of sensory neurons[5,6]. Only ciliated neurons express *osm-6::gfp*, with male-specific expression in four CEM head neurons and neurons of the rays and copulatory spicules[7]. Expression of *osm-6::gfp* begins at the L4 stage in neuronal cell bodies and extends to dendrites as neuronal outgrowth proceeds. The RnA and RnB neurons of each ray (rays 1–9), both HOA and HOB hook neurons, the spicule neurons SPV and SPD, and the PCB postcloacal sensilla neurons accumulate green fluorescent protein (GFP). OSM-6 may be required for the structure and function of ciliated neurons in the tail of the adult male, just as it is for neurons involved in many sensory behaviours[8,9].

By screening for mutants defective in vulva location, we identified *lov-1(sy552)*, which results in specific response and vulva-location

defects. When a *lov-1(+)* male encounters a hermaphrodite, it responds by placing its tail flush on the hermaphrodite, then backs along her body, and turns at her ends until it stops at her vulva. *lov-1* mutant males frequently fail to respond to hermaphrodite contact. Compared with the 88% responsiveness of wild-type males ($n = 82$), *sy552* male responsiveness is 24% ($n = 37$, $P < 0.0001$). When responsive is initiated, *lov-1(sy552)* mutants back and turn normally but frequently pass the vulva (Table 1), although spicule insertion and sperm transfer are unaffected. *lov-1(sy552)* males exhibit high mating efficiency with severely paralysed *unc-52* hermaphrodites, but sire few progeny with active, moving *dpy-17* hermaphrodites, presumably because a paralysed partner is an easy target, whereas an active partner evades the *lov-1* mutant male. *lov-1(sy552)* mutants appear normal for movement, egg-laying, nose touch, tap, mechanosensation and osmotic avoidance.

We cloned the *lov-1* gene on the basis of its genetic map position (Fig. 1). *sy552* is recessive. *mnDf21/sy552* and *sy552/sy552* males are phenotypically indistinguishable, so it is likely that *sy552* decreases the function of *lov-1*. *lov-1* falls between the breakpoints of *eDf21* and *mnDf21*. Cosmids in this region were injected and only ZK945 rescued *lov-1* defects (4 out of 5 stable lines). A 16.9-kilobase (kb) subclone (plov-1.1) rescued both the response and vulva-location defects of *sy552*, but shorter subclones did not (Fig. 1). Both a 6.7-kb (plov-1::gfp1) and a plov-1.1 frameshirt clone (plov-1.3) failed to rescue *sy552* defects, yet dominantly inhibited vulva location but not response (Fig. 1).

lov-1 encodes a predicted 3,125-amino-acid membrane-bound protein with a serine–threonine-rich, potential extracellular domain similar to mucins[3], a polycystin homology block 1 (26% identity), and a carboxy-terminal polycystin block 2 with 20% identity to polycystin proteins 1, 2 and 2L, encoded by the PKD1, PKD2 and PKDL loci, respectively (Fig. 2). A Kyte–Doolittle hydropathy plot predicts several transmembrane domains. No signal peptide is predicted in LOV-1. Mutations in PKD1 or PKD2 account for 95% of autosomal dominant polycystic disease[4]. There is similarity between LOV-1, the polycystins and the TRP and voltage-activated calcium and potassium family of channels in the transmembrane spanning region[10–14]. LOV-1 lacks the Ca^{2+}-binding EF-hand of polycystins 2 and L, the characteristic pore region of channels, and a cytoplasmic coiled-coil tail of all three polycystins (Fig. 2), which mediate hetero- and homotypic interactions between polycystin 1 and polycystin 2 (refs 15, 16). However, truncation of 58 C-terminal amino acids of LOV-1 (LOV-1::GFP5) destroys its function (Fig. 1), indicating that the LOV-1 cytoplasmic tail may be important for LOV-1 action. LOV-1 possesses a potential nucleotide-binding domain (Fig. 2) not present in the human polycystins. Polycystins have recently been implicated in signal transduction[17–19]. Consistent with a signalling function, PKD2 and the TRPC1 channel interact *in vitro*, as do PKD1 and TRPC family members[20].

We isolated *sy582Δ*, a genomic deletion of *lov-1* that encodes a truncated protein lacking the polycystin/channel homology domain (Fig. 1). *lov-1(sy582Δ)* has a similar genetic and phenotypic profile to *sy552* (Table 1). *sy552/sy582Δ* males are phenotypically indistinguishable from *sy552/Df* males, consistent with *sy582Δ* being a null allele. Thus, the polycystin block 2 is required for LOV-1 activity.

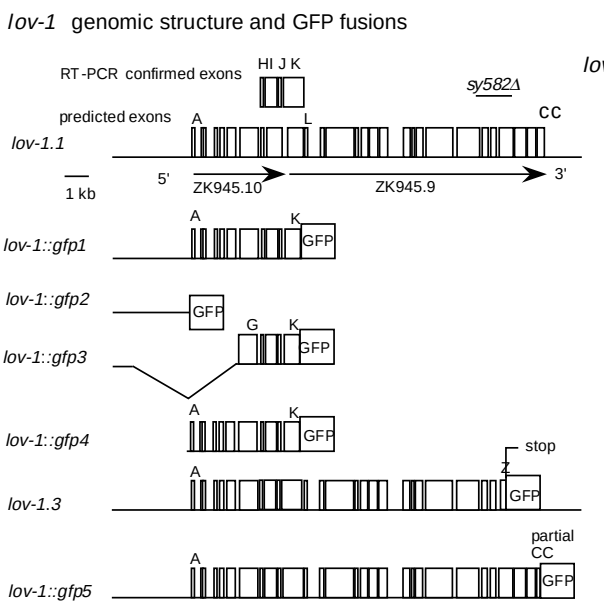

	Behavioural phenotypes		Expression pattern	Subcellular localization
	lov-1(sy552) rescue	wild type	wild type	
lov-1.1	+ (6/8)	+		
lov-1::gfp1	- (0/2)	DN	male-specific sensory neurons: CEMs, HOB, rays	Basodendritic (Cell body, sensory ending)
lov-1::gfp2		+	faint, nonspecific	
lov-1::gfp3		+	faint, male-specific: 1 or 2 unid'ed neurons	
lov-1::gfp4		+	faint, nonspecific	
lov-1.3	- (0/2)	DN	not expressed	
lov-1::gfp5	- (0/3)	+	male-specific sensory neurons: CEMs, HOB, rays	Cell body only
pkd-2::gfp1	-	+	male-specific sensory neurons: CEMs, HOB, rays nonspecific, ring neurons (weak)	Uniform (cell body, axon, dendrite)
pkd-2::gfp2	-	+	male-specific sensory neurons: CEMs, HOB, rays	Basodendritic (Cell body, sensory ending)

Figure 1 *lov-1* and *pkd-2* genomic structures, constructs, rescue data and expression patterns. The line above the *lov-1* gene indicates the 1,055-bp deletion in *lov-1(sy582Δ)*. Numbers in parentheses indicate the ratio of rescuing stable lines to the number of total stable lines examined. DN, dominant negative.

We examined the expression pattern of LOV-1::GFP reporters. A 6.7-kb fusion (LOV-1::GFP1) and a 15.4-kb fusion lacking only 58 amino acids (LOV-1::GFP5) direct expression in male-specific sensory neurons (Figs 1 and 3). Shorter versions of *lov-1::gfp1* are not expressed in the same set of male-specific neurons, nor do they act as dominant negatives (Fig. 1). *lov-1::gfp1* and *lov-1::gfp5* are expressed in male-sensory neurons, specifically the CEM neurons, the hook neuron HOB, and the sensory ray neurons. Expression begins during late L4 lethargus and peaks in the adult male. LOV-1::GFP1 is localized at high levels in the cell body (punctate cytoplasmic expression) and ciliated endings (Fig. 3), whereas LOV-1::GFP5 is found exclusively in cell bodies. The temporal and spatial regulation of *lov-1* is concordant with its role in adult male mating behaviour. Rays mediate responses to contact with a hermaphrodite[2], the hook mediates vulva location[2], and the CEMs may be involved in chemosensation[5].

The functions of the polycystins and the molecular basis of kidney cystogenesis are not known, but polycystin 1 and polycystin 2 have been proposed to function in concert[4]. The *C. elegans* genome contains a PKD2 homologue with 27% overall identity (Fig. 2). Like PKD2, PKD-2 possesses six membrane-spanning domains, a positively charged fourth membrane-spanning segment, a pore region and the coiled-coil domain of all polycystins. PKD-2 is localized to the same male-specific sensory neurons as LOV-1 (Figs 1 and 3). Rarely, very faint non-sex- and non-stage-specific expression of *pkd-2::gfp1* is observed in nerve-ring cell bodies. Expression of *pkd-2::gfp1* (which lacks transmembrane domains) is uniform throughout the HOB, ray and CEM neurons. In contrast, the basodendritic localization of PKD-2::GFP2 (which contains membrane-spanning regions) is identical to that of LOV-1::GFP1 (Figs 1 and 3). If the expression patterns of *lov-1::gfp1* and *pkd-2::gfp2* do indicate protein localization, then the basodendritic localization of LOV-1 and PKD-2 is consistent with plasma-membrane localization and a role for polycystins in maintaining cell polarity[21]. Although GFP localization might not reflect protein localization, and subcellular protein localization remains ambiguous, LOV-1 and PKD-2 are colocalized to male-specific sensory neurons and so might function in the same pathway.

Although we cannot rule out a subtle developmental defect, the following lines of evidence suggest that LOV-1 has a sensory function. The rays of many cilium-structure mutants ectopically fill with FITC[9] but this defect is not observed in *lov-1(sy552)*. By using a functional OSM-6::GFP fusion protein to image sensory neurons, we found that *lov-1* sensory endings appear structurally normal. Also, LOV-1::GFP1 and PKD-2::GFP2 are not mislocalized in *lov-1* mutants suggesting that their neuronal structure is intact. Expression of *lov-1::gfp* peaks in the adult male, as opposed to expression of *osm-6::gfp*, which begins about the time of neuronal outgrowth. Furthermore, the CEMs are formed during embryogenesis, whereas expression of *lov-1::gfp* in the CEMs is strictly restricted to L4 lethargus and adulthood. Finally, scanning electron microscope and Normarski images show that hook and ray structures are normal.

Chemosensation and mechanosensation are probably involved in vulva location (M.B. and P.S., manuscript in preparation). Because mechanosensory mutant males are not defective in response or vulva location, these behaviours may be mediated by a set of gene products other than those involved in body-touch mechanosensation. LOV-1 might act in a sensory signalling pathway, coupling voltage-activated signalling or store-operated conductance in a similar way to hair-cell mechanosensation[22] and touch resonse in *C. elegans*[23] or light-induced cation conductance in *Drosophila* photoreceptor cells[24], respectively. Alternatively, LOV-1 might function as a molecular scaffold for other molecules, such as PKD-2, in establishing or maintaining neuronal cell polarity, or ultrastructurally in the assembly of male-specific cilia. □

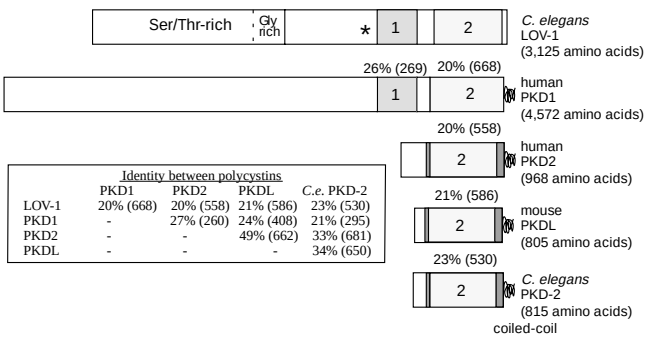

Figure 2 LOV-1 structural features and homologies. The LOV-1 N terminus is serine/threonine rich with several potential glycosylation sites followed by an ATP/GTP-binding domain (asterisk) and two polycystin blocks of homology. Block 2 also shows homology with voltage-activated Ca^{2+}-channel and TRP-channel families. The number of identical amino acids between LOV-1 and a particular polycystin is indicated. A coiled-coil is predicted in the middle of LOV-1, using the most stringent criteria for the COILS program. PKD-2 was identified in a BLAST search of unpublished sequences available through the Sanger Centre. A partial corresponding cDNA, yk219e1, was sequenced and aligned to the Genefinder ORFs Y73F8a.b and Y73F8a.a, changing the predicted size of PKD-2 from 913 to 815 amino acids. PKD-2 is more similar to PKD2 (33% identity, 52% similarity, 8% gaps over 681 amino acids) than LOV-1 (22% identity, 42% similarity, 13% gaps over 530 amino acids). Additional similarity between PKD2, PKD2L and PKD-2 is denoted by a hatching. Overall identity between polycystins, LOV-1 and PKD-2 is indicated.

Table 1 Vulva-location behaviour of wild-type and mutant males

Genotype	Vulva location efficiency (%)	Significantly different from wild-type	(*P*-value)	Number of males
him-5 (wild type)	96			101
osm-1(e1803)	65	No	(0.0738)	6
daf-10(p821)	48	Yes	(0.0004)	7
osm-5(p813); him-5	26	Yes	(0.0002)	5
osm-6(p811)	32	Yes	(0.0003)	7
che-3(e1124)	69	Yes	(0.02666)	4
lov-1(sy582Δ)	33	Yes	(<0.0001)	11
lov-1(sy552); him-5	30	Yes	(<0.0001)	73

lov-1(sy552); him-5(e1490), *lov-1(sy582Δ)* and all cilia-defective mutants were also response-defective. Males that eventually responded were scored for vulva-location behaviour. Males were observed for a minimum of 10 vulva encounters or until spicule insertion, whichever occurred first. Mann–Whitney tests determined *P*-values. the following mutants were also examined and found to be normal for resonse and vulva location: *osm-3(e1806); him-5*, *osm-7(n1515)*, *osm-8(n1518)*, *osm-10(n1602)*, *osm-11(n1604)*, *osm-12(n1606)*, *mec-3(e1338) him-8(e1489)*, *mec-4(e1611)*, *mec-5(e1340)*, *mec-7(n434)*, *mec-7(e343)*, *mec-8(e398)*, *mec-9(e1494)*, *che-1(e1034)*, *che-12(e1812)*, *odr-1(n1936)*, *odr-2(n2145)*, *odr-3(n2150)*, *odr-4(n2144ts)*, *odr-5(ky9)*, *odr-6(ky1)*, *odr-7(ky4)*, *odr-10(ky32)* and *daf-11(m47ts)*.

Methods

Mating efficiency and mating behaviour

Standard assays were performed using hermaphrodite strains N2, *unc-52 (e444)*, *dpy-17(e164)*, and *unc-31(e169)* with *him-5*(1490) or heat-shock-generated males[2,25,26]. Responsiveness reflects the percentage of males successfully responding to hermaphrodite contact within 10 min. An individual male's vulva-location ability was calculated as the number of positive vulva locations divided by the total number of vulva encounters. Vulva-location efficiency indicates the average behaviour of a genotypic population. Pairwise comparisons were made using Mann-Whitney nonparametric and two-sided *t*-tests.

Genetic screen for and mapping of *lov-1*

An F_2 clonal screen of EMS mutagenized PS1395 hermaphrodites [*plg-1(e2001d); him-5*][27] (K. Liu and P.S., unpublished) identified *lov-1(sy552)*. Mapping was performed using standard methods. From *unc-4(e120) let-25(mn25)* crosses, the *sy552* genotype was screened by complementation. Of 12 Unc non-Let recombinants, 2 segregate the *lov-1* mutant phenotype.

Transformation rescue of *lov-1(sy552)* mutants

Cosmids and plasmids (15–100 ng μl^{-1}) in the region from the right breakpoint of *eDf21* to the right breakpoint of *mnDf21* and PHA-1 (100 ng μl^{-1} pBX) was injected into *lov-1(sy552); pha-1(e2123ts); him-5*. Stable lines were selected at either 19 or 25 °C (ref. 28). A 16.9-kb *Hin*dIII fragment of ZK945 was cloned into pBS(SK+) (plov1.1). A frameshift in plov1.1 was created at nucleotide 17724 of ZK945 by inserting a *Bss*HII GFP fragment

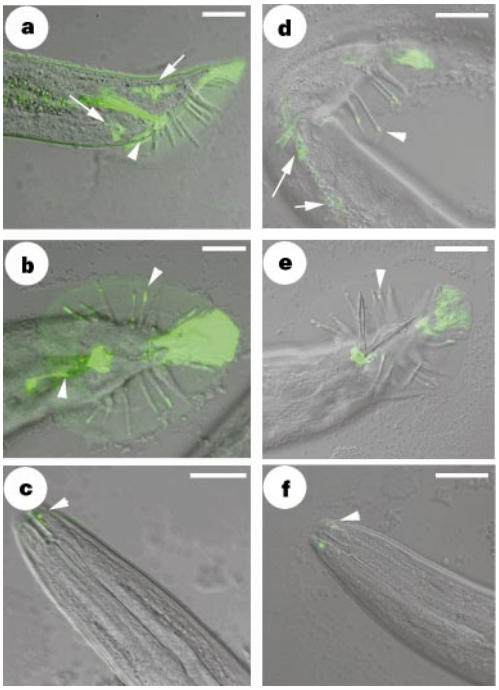

Figure 3 LOV-1::GFP1 and PKD-2::GFP2 are colocalized to adult male sensory-neuron cell bodies and dendrites. The spicules, hook structure and posteriormost fan region autofluoresce. Arrows, neuronal cell bodies; arrowheads, dendrites or ciliated endings. Images (merged DIC and fluorescence) were obtained using confocal microscopy. **a**–**c**, *lov-1::gfp1*. **a**, HOB and ray cell bodies (arrows), HOB dendritic process (arrowhead). **b**, HOB and ray process 5 (arrowheads). **c**, Ciliated endings in nose tip from male-specific cephalic CEM neurons (cell bodies not shown). **d**–**f**, *pkd-1::gfp2*. **d**, Ray cell bodies (arrow) and ray process 2 (arrowhead). **e**, Ray process 5 (arrowhead). **f**, Male-specific cephalic CEM ciliated endings (arrow). Scale bar, 20 μm.

from plasmid pPD95.02 (A. Fire, personal communication) out of frame into the *Stu*I site of plov-1.1, creating plov-1.3.

PCR screen for genomic deletion of *lov-1*

We followed the procedure of G. Moulder and R. Barstead (personal communication) and screened approximately 315,000 haploid genomes by using primers designed to delete the PKD/channel domain. *lov-1(sy582Δ)* deletes nucleotides 16972–18027 of ZK945.

DNA-sequence analysis

DNA sequence analysis of cDNA clones generated by RT-PCR from *him-5(e1490)* RNA revealed three exons in the junction between ZK945.10 and ZK945.9: one from 25742–25195, a second from 25151–25071, and a third initiating at position 25021, corresponding to exons I, J and K, in Fig. 1, respectively. Sequencing of the partial *pkd-2* cDNA yk219e indicates coding regions of Y73F8A.b and Y73F8A.a at 4932–4480, 3813–3562, 3400–3147, 2100–1972, and 1692–1606.

Expression analysis

GFP[29] was used as a marker for *lov-1* and *pkd-2* gene expression. plov-1::GFP1 was constructed by cloning a 6.7-kb *Hin*dIII–*Bam*H1 fragment of plov-1.1 into the vector pPD95.81, plov-1::GFP2 a *Hin*dIII-*Hpa*I fragment. plov-1::GFP3 and plov-1::GFP4 are *Sac*I and *Hin*dIII–*Hpa*I (Klenow filled-in and relegated) deletions of plov-1::GFP1, respectively. plov-1::gfp5 was constructed by cloning a 15.4-kb *Hin*dIII–*Afe*I fragment of plov-1.1 into the *Hin*dIII–*Sma*I site of pPD95.79. ppkd-2.1, ppkd-2::gfp1 and ppkd-2::gfp2 were constructed by cloning PCR-amplified 8.9-kb, 2.0-kb and 5.9-kb fragments into the vectors pPD.95.97, pPD95.75 and pPD95.77, respectively. Cells were identified by comparing Nomarski and fluorescent or confocal images of the same animals to determine cell-body position[30]. HOB assignment was confirmed by laser ablation of precursor cells.

Received 23 April; accepted 16 July 1999.

1. Hodgkin, J. in *The Nematode* C. elegans (ed. Wood, B.) 243–279 (Cold Spring Harbor Laboratory Press, New York, 1988).
2. Liu, K. S. & Sternberg, P. W. Sensory regulation of male mating behavior in *Caenorhabditis elegans*. *Neuron* **14,** 79–89 (1995).
3. Carraway, K. L. & Fregien, N. Mucin structure and function: Insights from molecular biology. *Trends Glycosci. Glycotechnol.* **7,** 31–44 (1995).
4. Torres, V. D. New insights into polycystic kidney disease and its treatment. *Curr. Opin. Nephrol. Hypertens.* **7,** 159–169 (1998).
5. Ward, S., Thomson, N., White, J. G. & Brenner, S. Electron microscopical reconstruction of the anterior sensory anatomy of the nematode *Caenorhabditis elegans*. *J. Comp. Neurol.* **160,** 313–337 (1975).
6. White, J. G., Southgate, D., Thomson, J. N. & Brenner, S. The structure of the nervous system of *Caenorhabditis elegans*. *Phil. Trans. R. Soc. Lond. B* **314,** 1–340 (1986).
7. Collet, J., Spike, C. A., Lundquist, E. A., Shaw, J. E. & Herman, R. K. Analysis of *osm-6*, a gene that affects sensory cilium structure and sensory neuron function in *Caenorhabditis elegans*. *Genetics* **148,** 187–200 (1998).
8. Kaplan, J. M. & Horvitz, H. R. A dual mechanosensory and chemosensory neuron in Caenorhabditis elegans. *Proc. Natl Acad. Sci. USA* **90,** 2227–2231 (1993).
9. Perkins, L. A., Hedgecock, E. M., Thomson, J. N. & Culotti, J. G. Mutant sensory cilia in the nematode *Caenorhabditis elegans*. *Dev. Biol.* **117,** 456–487 (1986).
10. Mochizuki, T. *et al.* PKD2, a gene for polycystic kidney disease that encodes an integral membrane protein. *Science* **242,** 1339–1342 (1996).
11. Montell, C. & Rubin, G. M. Molecular characterization of the *Drosophila trp* locus: a putative integral membrane protein required for phototransduction. *Neuron* **2,** 1313–1323 (1989).
12. Sanford, R. *et al.* Comparative analysis of the polycystic kidney disease 1 (PKD1) gene reveals an integral membrane glycoprotein with multiple evolutionary conserved domains. *Hum. Mol. Genet.* **9,** 1483–1489 (1997).
13. Nomura, H. *et al.* Identification of PKDL, a novel polycystic kidney disease 2-like gene whose murine homologue is deleted in mice with kidney and retinal defects. *J. Biol. Chem.* **273,** 25967–25973 (1998).
14. Wu, G. *et al.* Identification of PKD2L, a human PKD2-related gene: Tissue-specific expression and mapping to chromosome 10q25. *Genomics* **54,** 564–568 (1998).
15. Qian, F. *et al.* PKD1 interacts with PKD2 through a probably coiled-coil domain. *Nature Genet.* **16,** 179–183 (1997).
16. Tsiokas, L., Kim, E., Arnould, T., Sukhatme, V. P. & Walz, G. Homo- and heterodimeric interactions between the gene products of PKD1 and PKD2. *Proc. Natl Acad. Sci. USA* **94,** 6965–6970 (1997).
17. Arnould, T. *et al.* The polycystic kidney disease 1 gene product mediates protein kinase C α-dependent and c-Jun N-terminal kinase-dependent activation of the transcription factor AP-1. *J. Biol. Chem.* **273,** 6013-6018 (1998).
18. Parnell, S. C. *et al.* The polycystic kidney disease-1 protein, polycystin-1, binds and activates heterotrimeric G-proteins *in vitro*. *Biochem. Biophys. Res. Commun.* **251,** 625–631 (1998).
19. Kim, E. *et al.* The polycystic kidney kidney disease 1 gene product modulates Wnt signaling. *J. Biol. Chem.* **274,** 4947–4953 (1999).
20. Tsiokas, L. *et al.* Specific association of the gene product of PKD2 with the TRPC1 channel. *Proc. Natl Acad. Sci. USA* **7,** 3934–3939 (1999).
21. Sullivan, L. P., Wallace, D. P. & Grantham, J. J. Epithelial transport in polycystic kidney disease. *Physiol. Rev.* **78,** 1165–1191 (1998).
22. Hudspeth, A. J. How the ear's works work. *Nature* **341,** 397–404 (1989).
23. Driscoll, M. & Kaplan, J. in C. elegans *II* (ed. Riddle, D. I., Blumenthal, T., Meyer, B. J. & Priess, J. R.) 645–677 (Cold spring Harbor Laboratory Press, New York, 1997).
24. Montell, C. TRP trapped in the fly signalling web. *Curr. Opin. Neurobiol.* **8,** 389–397 (1998).
25. Brenner, S. The genetics of *Caenorhabditis elegans*. *Genetics* **77,** 71–94 (1974).
26. Hodgkin, J. Male phenotypes and mating efficiency in *Caenorhabditis elegans*. *Genetics* **103,** 43–64 (1983).
27. Hodgkin, J. & Doniach, T. Natural variation and copulatory plug formation in *Caenorhabditis elegans*. *Genetics* **146,** 149–164 (1997).
28. Schnabel, H. & Schnabel, R. An organ-specific differentiation gene, *pha-1*, from *Caenorhabditis elegans*. *Science* **250,** 686–688 (1990).
29. Chalfie, M., Tu, Y., Euskirchen, G., Ward, W. W. & Prasher, D. D. Green fluorescent protein as a marker for gene expression. *Science* **263,** 802–805 (1994).
30. Sulston, J. D., Albertson, D. G. & Thomson, J. N. The *Caenorhabditis elegans* male: Postembryonic development of nongonadal structures. *Dev. Biol.* **78,** 542–576 (1980).

Acknowledgements

We thank J. Copeland for help isolating *lov-1(sy582Δ)*; L. Jiang, R. Garcia and R. Ballester for discussions and constructive criticisms; members of our lab, S. Myers and M. Snow for experimental suggestions; D. Sherwood and B. Smith for assistance with confocal microscopy; A. Fire for vectors; and R. Herman for *osm-6::gfp*. The Caenorhabditis Genetics stock Center and Sanger Center provided numerous strains, cosmids and sequencing data. This work was supported by the Howard Hughes Medical Institute, with which P.W.S. is an investigator and M.M.B. is an associate, and by the Seaver Institute.

Correspondence and requests for materials should be addressed to P.W.S. (e-mail: pws@cco.caltech.edu).